

Temporal changes of human cone photoreceptors observed in vivo with SLO/OCT

M. Pircher,^{1,*} J. S. Kroisamer,^{1,2} F. Felberer,¹ H. Sattmann,¹ E. Götzinger,¹
and C. K. Hitzenberger¹

¹Center for Medical Physics and Biomedical Engineering, Medical University of Vienna, Waehringerstr. 13,
1090 Vienna, Austria

²Department of Ophthalmology and Optometry, Medical University of Vienna, Waehringerguertel 18-20,
1090 Vienna, Austria

*michael.pircher@meduniwien.ac.at

Abstract: In this study we use our previously introduced scanning laser ophthalmoscope (SLO) / transverse scanning optical coherence tomography (TS-OCT) instrument to investigate long term changes in cone photoreceptors. The instrument is capable to provide 3D information of the human cone photoreceptors with negligible eye motion artifacts due to an implemented 3D motion correction on a cellular level. This allows for an in vivo investigation of exactly the same location on the retina with cellular resolution over several days. Temporal changes in the backscattered intensity are observed and quantified within the junction between inner and outer segments of cone photoreceptors, the cone outer segments, the end tips of cone photoreceptors and the retinal pigment epithelium. Furthermore, the length of individual cone outer segments is measured and observed over time. We show, to the best of our knowledge for the first time, that bright reflection spots which are located within the outer segment of cone photoreceptors change their position when observed over extended time periods. The average measured bright reflection spot motion speed corresponds well to the expected cone growth speed. We believe that this observation can be associated with the first direct in vivo imaging of the cone renewal process.

©2010 Optical Society of America

OCIS codes: (170.4500) Optical coherence tomography; (330.5310) Vision – photoreceptors; (170.5755) Retina scanning; (170.4470) Ophthalmology; (170.2655) Functional monitoring and imaging.

References and links

1. R. J. Zawadzki, S. M. Jones, S. S. Olivier, M. T. Zhao, B. A. Bower, J. A. Izatt, S. Choi, S. Laut, and J. S. Werner, "Adaptive-optics optical coherence tomography for high-resolution and high-speed 3D retinal in vivo imaging," *Opt. Express* **13**(21), 8532–8546 (2005).
2. J. Z. Liang, D. R. Williams, and D. T. Miller, "Supernormal vision and high-resolution retinal imaging through adaptive optics," *J. Opt. Soc. Am. A* **14**(11), 2884–2892 (1997).
3. A. Roorda, and D. R. Williams, "The arrangement of the three cone classes in the living human eye," *Nature* **397**(6719), 520–522 (1999).
4. A. Roorda, F. Romero-Borja, W. Donnelly Iii, H. Queener, T. J. Hebert, and M. C. W. Campbell, "Adaptive optics scanning laser ophthalmoscopy," *Opt. Express* **10**(9), 405–412 (2002).
5. M. Pircher, R. J. Zawadzki, J. W. Evans, J. S. Werner, and C. K. Hitzenberger, "Simultaneous imaging of human cone mosaic with adaptive optics enhanced scanning laser ophthalmoscopy and high-speed transversal scanning optical coherence tomography," *Opt. Lett.* **33**(1), 22–24 (2008).
6. D. T. Miller, D. R. Williams, G. M. Morris, and J. Z. Liang, "Images of cone photoreceptors in the living human eye," *Vision Res.* **36**(8), 1067–1079 (1996).
7. C. Torti, B. Povazay, B. Hofer, A. Unterhuber, J. Carroll, P. K. Ahnelt, and W. Drexler, "Adaptive optics optical coherence tomography at 120,000 depth scans/s for non-invasive cellular phenotyping of the living human retina," *Opt. Express* **17**(22), 19382–19400 (2009).
8. C. A. Curcio, K. R. Sloan, R. E. Kalina, and A. E. Hendrickson, "Human photoreceptor topography," *J. Comp. Neurol.* **292**(4), 497–523 (1990).

9. M. Pircher, B. Baumann, E. Götzinger, and C. K. Hitzenberger, "Retinal cone mosaic imaged with transverse scanning optical coherence tomography," *Opt. Lett.* **31**(12), 1821–1823 (2006).
10. B. Potsaid, I. Gorczynska, V. J. Srinivasan, Y. L. Chen, J. Jiang, A. Cable, and J. G. Fujimoto, "Ultra-high speed spectral / Fourier domain OCT ophthalmic imaging at 70,000 to 312,500 axial scans per second," *Opt. Express* **16**(19), 15149–15169 (2008).
11. R. W. Young, "The renewal of photoreceptor cell outer segments," *J. Cell Biol.* **33**(1), 61–72 (1967).
12. R. W. Young, and D. Bok, "Participation of the retinal pigment epithelium in the rod outer segment renewal process," *J. Cell Biol.* **42**(2), 392–403 (1969).
13. D. H. Anderson, S. K. Fisher, and R. H. Steinberg, "Mammalian cones: disc shedding, phagocytosis, and renewal," *Invest. Ophthalmol. Vis. Sci.* **17**(2), 117–133 (1978).
14. B. M. Kevany, and K. Palczewski, "Phagocytosis of retinal rod and cone photoreceptors," *Physiology (Bethesda)* **25**(1), 8–15 (2010).
15. R. S. Jonnal, J. R. Besecker, J. C. Derby, O. P. Kocaoglu, B. Cense, W. H. Gao, Q. Wang, and D. T. Miller, "Imaging outer segment renewal in living human cone photoreceptors," *Opt. Express* **18**(5), 5257–5270 (2010).
16. M. Pircher, E. Götzinger, H. Sattmann, R. A. Leitgeb, and C. K. Hitzenberger, "In vivo investigation of human cone photoreceptors with SLO/OCT in combination with 3D motion correction on a cellular level," *Opt. Express* **18**(13), 13935–13944 (2010).
17. M. Pircher, B. Baumann, E. Götzinger, H. Sattmann, and C. K. Hitzenberger, "Simultaneous SLO/OCT imaging of the human retina with axial eye motion correction," *Opt. Express* **15**(25), 16922–16932 (2007).
18. P. Thévenaz, U. E. Ruttimann, and M. Unser, "A pyramid approach to subpixel registration based on intensity," *IEEE Trans. Image Process.* **7**(1), 27–41 (1998).
19. A. Pallikaris, D. R. Williams, and H. Hofer, "The reflectance of single cones in the living human eye," *Invest. Ophthalmol. Vis. Sci.* **44**(10), 4580–4592 (2003).
20. J. L. Schnapf, T. W. Kraft, and D. A. Baylor, "Spectral sensitivity of human cone photoreceptors," *Nature* **325**(6103), 439–441 (1987).
21. B. Cense, E. Koperda, J. M. Brown, O. P. Kocaoglu, W. H. Gao, R. S. Jonnal, and D. T. Miller, "Volumetric retinal imaging with ultrahigh-resolution spectral-domain optical coherence tomography and adaptive optics using two broadband light sources," *Opt. Express* **17**(5), 4095–4111 (2009).
22. R. J. Zawadzki, B. Cense, Y. Zhang, S. S. Choi, D. T. Miller, and J. S. Werner, "Ultra-high-resolution optical coherence tomography with monochromatic and chromatic aberration correction," *Opt. Express* **16**(11), 8126–8143 (2008).
23. C. J. Guérin, G. P. Lewis, S. K. Fisher, and D. H. Anderson, "Recovery of photoreceptor outer segment length and analysis of membrane assembly rates in regenerating primate photoreceptor outer segments," *Invest. Ophthalmol. Vis. Sci.* **34**(1), 175–183 (1993).
24. D. H. Anderson, S. K. Fisher, P. A. Erickson, and G. A. Tabor, "Rod and cone disc shedding in the rhesus monkey retina: a quantitative study," *Exp. Eye Res.* **30**(5), 559–574 (1980).
25. G. A. Tabor, S. K. Fisher, and D. H. Anderson, "Rod and cone disc shedding in light-entrained tree squirrels," *Exp. Eye Res.* **30**(5), 545–557 (1980).
26. R. W. Young, "The daily rhythm of shedding and degradation of rod and cone outer segment membranes in the chick retina," *Invest. Ophthalmol. Vis. Sci.* **17**(2), 105–116 (1978).
27. R. W. Young, "Daily rhythm of shedding and degradation of cone outer segment membranes in lizard retina," *J. Ultrastructure Res.* **61**, 172–185 (1977).
28. W. T. O'Day, and R. W. Young, "Rhythmic daily shedding of outer-segment membranes by visual cells in the goldfish," *J. Cell Biol.* **76**(3), 593–604 (1978).

1. Introduction

Vision is one of the most complex of human senses. The incoming light is converted into electrical signals by the retina which performs a preprocessing of the information before it is finally sent to the brain. The retina consists of millions of photosensitive cells that can be divided into two categories: Rods that enable scotopic vision and cones that enable photopic vision. While rods are still very hard to resolve with modern image technologies, several different techniques have been reported that are capable to resolve individual cones [1–7]. However, the cone density varies considerably throughout the retina which shows the highest density in the fovea and decreases with eccentricity from the fovea [8]. Therefore individual cones can be resolved in many subjects even without compensation of aberrations introduced by imperfections of the eye optics using adaptive optics when the imaged location on the retina is sufficiently far from the fovea [6,9,10].

The outer segments (OS) of human cone photoreceptors consist of a stack of membrane disks that contain the photo-pigments. To minimize damage by photo-toxic processes the OS undergo changes with time. These changes include the formation of new disks at the junction between inner and outer segments of photoreceptors and disk shedding followed by

phagocytosis of these shed disks at the border between photoreceptors and the retinal pigment epithelium (RPE) [11–13]. These processes have been studied extensively in vitro in animal experiments and differing changes can be observed not only from species to species but also between rods and cones [14]. However, in vivo assessment of these changes is still very challenging. Only very recently the cone outer segment renewal rate was measured indirectly in vivo using an adaptive optics equipped fundus camera (AO-FC) [15]. In this specific AO-FC setup the retina is illuminated with a temporally coherent light source. By assuming that only reflections of the junction between inner and outer segments of cone photoreceptors (IS/OS) and end tips of photoreceptors (ETPR) are contributing to the backscattered signal in the AO-FC system (the majority of the other layers will not contribute to the light intensity because of the narrow depth of focus) the light from both interfaces will interfere. Depending on the length of the outer segment, constructive or destructive interference is occurring which results in high or low signal intensity, respectively. By measuring the same location on the retina every 15 minutes, sinusoidal intensity oscillations can be observed. The frequency of this oscillation can be used to estimate the cone growth.

In this paper we introduce a different approach in order to investigate long term intensity changes as well as changes in the three dimensional structure of cone photoreceptors. We use our previously introduced transverse scanning optical coherence tomography (TS-OCT) / scanning laser ophthalmoscope (SLO) instrument that is capable to provide this 3D information with negligible eye motion artifacts due to an implemented 3D motion correction on a cellular level [16]. We evaluate structural changes as well as changes in the backscattered intensity from different interfaces of the cone photoreceptors. Recently, we reported on bright reflection spots (BRS) that can be observed within the outer segments (OS) of cone photoreceptors [16]. We demonstrate what we believe for the first time, that these BRS are changing their position during time periods of several days. We further hypothesize that the BRS correspond to defects within the OS disc stacking which can be used to observe directly the process of cone renewal in vivo.

2. Method

The principle of the TS-OCT/SLO instrument is published elsewhere [16,17]. In brief, the instrument is capable to record en-face OCT and SLO images simultaneously. The theoretical depth (in tissue) and transverse resolutions of the instrument are equal and about 4-5 μ m. The system is operated at a frame rate of 40 fps (200x650 pixels, $\sim 1^\circ \times 1^\circ$). A 3D data set (120 transverse scans, 200 μ m in depth) is recorded in 3 seconds. A hardware implemented high speed (~ 1 kHz) axial eye tracker ensures negligible axial eye motion artifacts (smaller than the depth resolution of the system). In a post-processing step the information from the simultaneously recorded SLO images is used to correct for transverse eye motion. This is achieved in two steps. In a first step a reference frame (with negligible motion artifacts) is chosen and all SLO frames are registered (via cross correlation using a custom made software) to this reference frame and averaged. In a second step the averaged frame is used as a new reference frame and the original SLO images are registered to this new reference frame. The transformation matrix for each SLO image is stored and applied to the OCT images in order to obtain a motion corrected 3D volume of the retina. However, the initial field of view is slightly reduced because of this procedure.

To minimize any influences of subject alignment on the measurement, 10 3D data sets were recorded at exactly the same location on the retina ($\sim 4^\circ$ eccentricity nasal from the fovea) of healthy volunteers for every time point in the time series. This specific eccentricity was chosen because of several reasons. First, the density of the BRS at this eccentricity is high [16]. Second, for the used system the contrast of the cone mosaic is very good and finally, the distance between individual cones is larger than the resolution of the system which ensures that all cones can be resolved. In order to register the 10 data sets to each other the averaged SLO frame of the first data set was stored and used as reference frame for all the other data

sets. Out of the 10 data sets those with the best image quality (a minimum of 5) were selected, registered in depth to each other and averaged. We used the following image quality parameters for this selection (ordered by relevance): field of view (after registration), micro-saccade within an extracted OCT B-scan, cone contrast and signal to noise ratio of the image. This procedure minimizes residual motion artifacts and differing image quality due to subject alignment. However, a residual rotation between data sets recorded at different times may occur. To eliminate this rotation, the final data sets were registered using Image J software [18]. It should be noted, however, that the observed rotations between the data sets were very small (resulting in a displacement between different data sets at the corners of the image of approximately the extension of a cone). In the case of larger rotations a different procedure (first separate registration within each data set, then registration between data sets) might be better suited. In order to adapt differing total intensities between measurements at different times, the intensity data of each data set was normalized by the total intensity of the data set.

All measurements were performed without an artificial pupil dilation of the subjects. For this experiment good fixation of the subject is essential. Therefore a fixation target (organic light emitting diode display) was coupled via a pellicle beam splitter into the system. The subject fixated on the target with the same eye that was measured. All measurements were approved by the local ethic committee and followed the tenets of the declaration of Helsinki.

3. Results

3.1. Short term measurement

In a first measurement series short term changes (within 7 hours, from 9 a.m. to 4 p.m.) are investigated. For this purpose at every hour 3D data sets were recorded up to a total time of 7 hours. At each measurement time a minimum of 10 data sets were recorded (within 5 minutes) resulting in a total of 80 data sets and processed as described above. Figure 1 shows a movie of a time series. Each frame consists of depth integrated (over the entire imaging depth) OCT images (left images) and averaged SLO images (right images). Although the measurements were taken over an extended period of time, the motion correction algorithm provides high registration accuracy between the individual 3D data sets (better than the extension of a single cone). Similar to a previously reported study with an adaptive optics ophthalmoscope [19] randomly varying intensities of individual cones can be observed in the time series of the SLO images (c.f. Figure 1). The depth integrated OCT images show the same intensity fluctuations. However, in our case the retina was not bleached prior to the measurement because we think that at the used wavelength region (840nm) intensity variations due to pigment absorbance are negligible. (Electrophysiology measurements on the retina showed that the photo-sensitivity of the cones is reduced by more than a factor of 10^5 at 840nm compared to the peak sensitivity of the red cones at 560nm [20]). We further want to point out that a short coherence light source is used for illumination, therefore the observed intensity fluctuations are distinct from intensity fluctuations that are observed with long coherence light sources (which were attributed to interferometric oscillations caused by sub micrometer outer segment length changes [15]). Since these fast oscillations are not observable with low coherent light sources [15,19] we chose the lower temporal sampling compared to that in Ref [15]. (1h vs. 15 Min.). Because of the perfect registration between the frames, averaging of the data sets recorded over the entire measurement period is possible which results in an image of the cone mosaic with reduced intensity fluctuations (c.f. Figure 2). Nevertheless, dark patches within the cone mosaic (apart from the shadow of the vessel in the top part of the image) are still remaining.

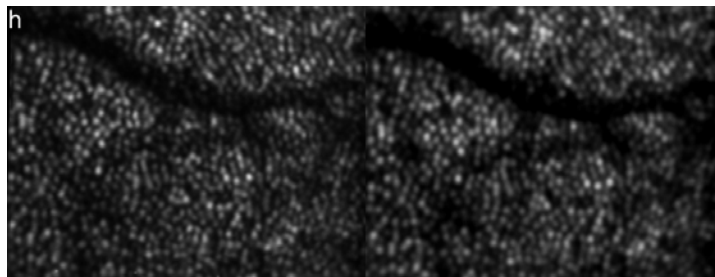


Fig. 1. First frame of a movie ([Media 1](#)) showing intensity fluctuations in depth integrated OCT (left) and SLO (right) images of cone photoreceptors within 7 hours (image extension: $\sim 0.94^\circ \times 0.7^\circ$, retinal eccentricity: $\sim 4^\circ$ nasal from the fovea)

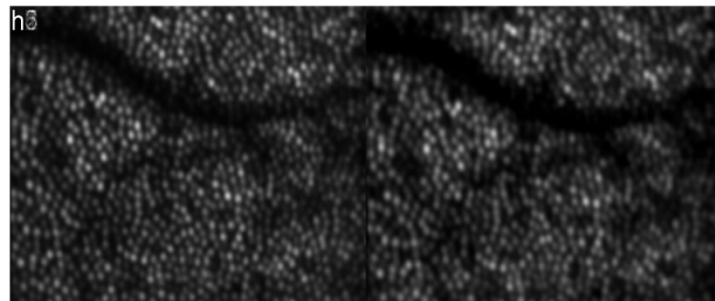


Fig. 2. Over the entire measurement period (7 hours) averaged depth integrated OCT and SLO images of cone photoreceptors demonstrating the excellent performance of the motion correction algorithm. (Image extension: $\sim 0.94^\circ \times 0.7^\circ$, retinal eccentricity: $\sim 4^\circ$ nasal from the fovea)

In contrast to a previous study performed with an adaptive optics ophthalmoscope we have access to the depth information provided by OCT. Figure 3 shows a movie of a representative B-scan measured over time.

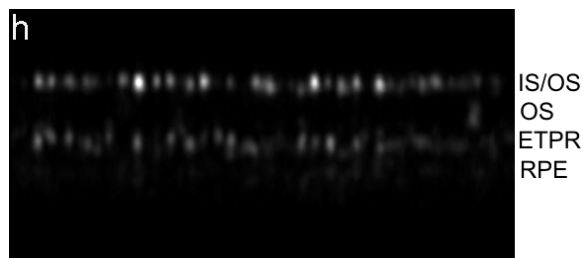


Fig. 3. Frame 1 of a movie ([Media 2](#)) showing a representative B-scan over the entire measurement period (7 hours). Image extension: $\sim 0.94^\circ \times 120\mu\text{m}$, retinal eccentricity: $\sim 4^\circ$ nasal from the fovea)

Note that the B-scans are displayed on a linear grey scale (contrary to the usual OCT log intensity scale); therefore only two layers, the junction between inner and outer segments of cone photoreceptors (IS/OS) and the end tips of cone photoreceptors (ETPR) are visible, however, the reflections from the cones can be much better observed. The retinal pigment epithelium (RPE) layer is hardly observable in this scale. Both layers show distinct spots that represent refractive index changes within single cone photoreceptors. As can be observed in the movie the spatial location of these spots do not change within the measurement period of 7 hours. However, most of the cones show intensity fluctuations either in the IS/OS or the ETPR layer. Interestingly these fluctuations seem to be independent from cone to cone and within the same cone from IS/OS junction to ETPR. Moreover, similar to the results reported

in Ref [19], the periodicity of the fluctuations is varying from cone to cone and between the two layers. Note that in the time series a distinct reflection at the transverse position of a cone within the RPE layer (brightest intensity is observed at h_5 at a cone in the center of the image) can be observed. These bright reflections have been observed previously with independent instruments [21,22]; however, this is the first time to show varying intensities and locations of these spots. The origin of these reflections is unclear but might be caused by backscattered light originating from the RPE that is back-coupled into a single cone. To give a better impression of the intensity fluctuations we segmented the layers IS/OS, OS, ETPR and RPE by summing the pixels over an imaging depth of $\sim 12\mu\text{m}$ around the center of the peak intensity of each layer (except for the OS layer where the gap between the segmented IS/OS and ETPR layers was integrated). The result is shown in Fig. 4. Interestingly, intensity variations can be observed within three layers (IS/OS, ETPR and RPE) while within the OS the intensity of the observed bright reflection spots stays rather constant. We reported and counted these BRS previously and showed that the amount of these BRS is differing with eccentricity from the fovea [16].

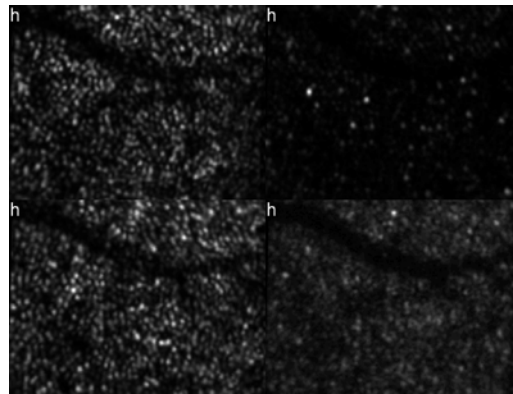


Fig. 4. Frame 1 of a movie (Media 3) showing intensity fluctuations at different retinal layers within the measurement period (7 hours). Top left: IS/OS. Top right: OS. Bottom left: ETPR. Bottom right: RPE. Image extension: $\sim 0.94^\circ \times 0.7^\circ$, retinal eccentricity: $\sim 4^\circ$ nasal from the fovea)

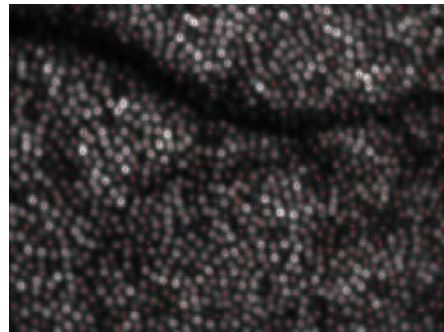


Fig. 5. Locations of the detected cones (marked with red dots).

In a next step we detected in the averaged OCT image (c.f. Figure 2, left image) the center of each cone with custom made software. Since the averaged image shows reduced intensity fluctuations between individual cones (in an individual frame some of the cones are hardly detectable because of low signal intensity) a good performance of the cone detection algorithm can be observed as is shown in Fig. 5 (each cone center is marked by a red dot). In this image series 884 cones were detected. In order to give an impression of the intensity fluctuations for individual cones in the depth integrated OCT intensity images we randomly

selected 5 cones and normalized the measured intensity at every hour with the mean intensity of the selected cone over the whole measurement series (c.f. Figure 6A). The majority of the cones show intensity fluctuations of ~50%. Additionally we measured for each cone the length of the outer segment (i.e. the distance from the IS/OS junction to the ETPR). Both interfaces are detected by using a peak detect algorithm along an A-scan at the location of the detected cone. As can be seen in Fig. 6B the outer segment length stays constant for 4 cones, whereas in one cone the length is much larger at two measurement points (5 and 7 hours). The length change of this one cone is an artifact generated by low signal intensity from the ETPR layer. In that case the algorithm uses the peak that is found within the RPE layer for the calculation of the outer segment length. Note that for the detection of the transverse cone position the depth integrated and averaged OCT data is used. Figure 7 shows a movie of the OS lengths for all detected cones. In the majority of the cones the OS length is detected correctly and stays constant over time which is also indicated in Fig. 8 which shows the distribution of cone outer segment lengths for all measurements. It is worth to note that the OS lengths vary from cone to cone (the distribution in Fig. 8 spans ~10 μ m) which can be observed in the B-scan images as well (c.f. Figure 3). The precision of our method to measure OS lengths is high as can be seen in Fig. 8B which shows the standard deviation of the individual cone OS length measurements at different times. For the majority of the cones the standard deviation is as small as ~1 μ m. This also indicates that the OS length measured with our technique does not change noticeable within this measurement period. We want to emphasize here that although the depth resolution of the system is ~4-5 μ m and the depth sampling is ~1.7 μ m (optical distance) per pixel, the peak of the coherence function can be determined with higher accuracy, because for peak detection a Gaussian fit is applied to the coherence function which results in a sub-pixel accuracy of the peak position. Our results are in agreement with animal studies [23,24] and recent measurements of the cone renewal rate that showed a cone growth rate of ~100nm per hour [15]. This results in an OS length change of less than 1 μ m for our 7 hour experiment.

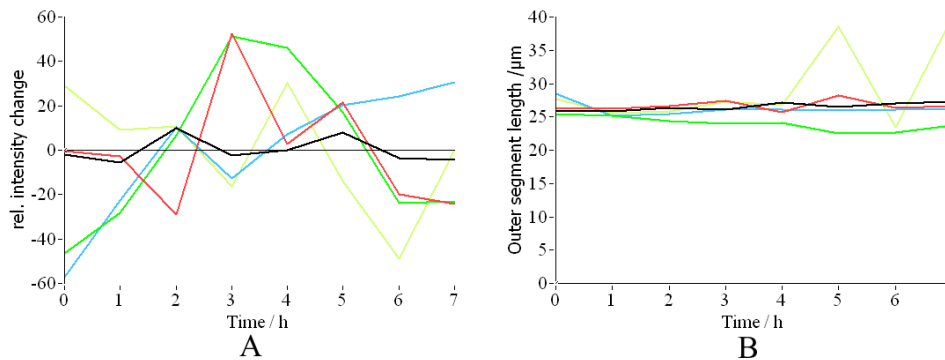


Fig. 6. A) Relative intensity changes with time of 5 randomly selected cones. B) Change in the measured length of cone outer segments.

To quantify the observed intensity changes we calculated the total distribution of the backscattered light at the location of the cones (c.f. Figure 9A) as well as the relative intensity changes over time for the individual retinal layers (c.f. Figure 9B). Although most of the cones show fluctuating backscattered intensities, the intensity distribution of all cones stays the same during the measurement period. As can be seen in Fig. 9B the fluctuations within each layer are much more pronounced than the total intensity fluctuations (c.f. black line in Fig. 9B). This indicates that the intensity fluctuations are probably not correlated between the individual layers. It should be noted, however, that the higher intensity fluctuations observed within the OS (green line) is caused by the low signal intensity observed at this layer at the majority of the cone locations. Only few cone locations show BRS within the OS [16].

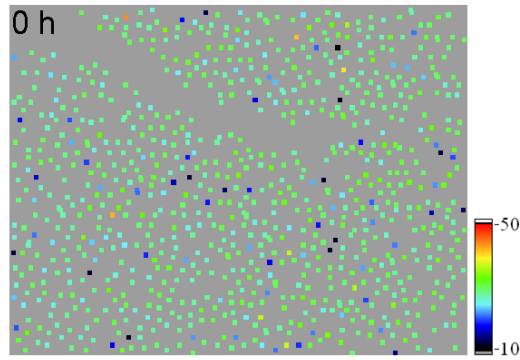


Fig. 7. Frame 1 of a movie (Media 4) showing outer segment lengths within the measurement period (7 hours). Image extension: $\sim 0.94^\circ \times 0.7^\circ$, retinal eccentricity: $\sim 4^\circ$ nasal from the fovea (color scale is in μm).

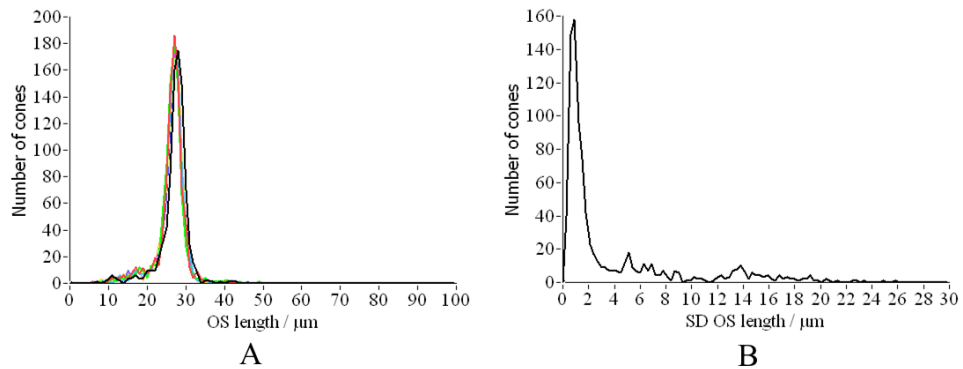


Fig. 8. A) Distribution of cone outer segment lengths for each hour (corresponding to different colors). B) Distribution of standard deviations calculated over the whole measurement period.

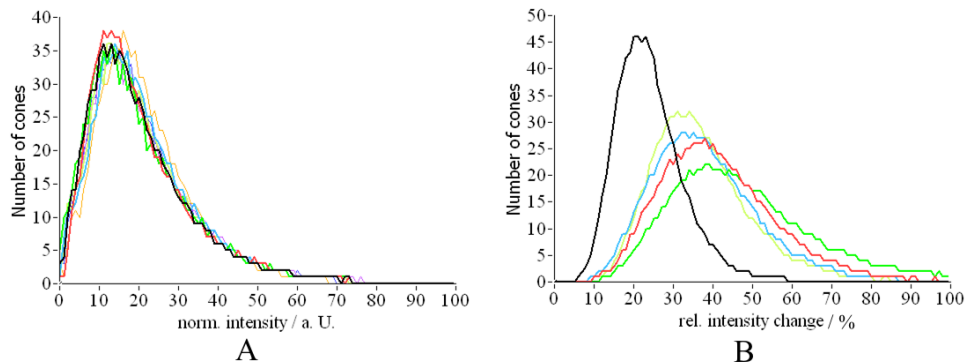


Fig. 9. A) Distribution of backscattered intensity of individual cones (colors correspond to different measurement times). B) Relative intensity variation (normalized by the average intensity retrieved from each layer) over time of cones for individual retinal layers (black depth integrated intensity, red IS/OS junction, green OS, blue ETPR, yellow RPE).

3.2 Long term measurement

In a second measurement series we measured two volunteers over an extended time period, i.e. every 24 hours up to a total time of 96 hours. The measurements were recorded at the same daytime (4p.m. in the afternoon). The subjects followed their normal daily schedule. The data was recorded and processed as described above. Figure 10 shows a movie over the

extend measurement period of OCT and SLO images from the same volunteer as in the first measurement series at approximately the same position (c.f. to the blood vessel in the top part of the image). Although the measurement was spread over five days the registration between the data sets is better than the extension of a single cone. Compared to the movie in Fig. 1 the intensity fluctuations are much more pronounced. To minimize the large differences between the cones in the backscattered intensity we averaged all images recorded over the whole measurement period before detecting the center of each cone (c.f. Figure 11). Here, again, dark patches within the cone mosaic are remaining.

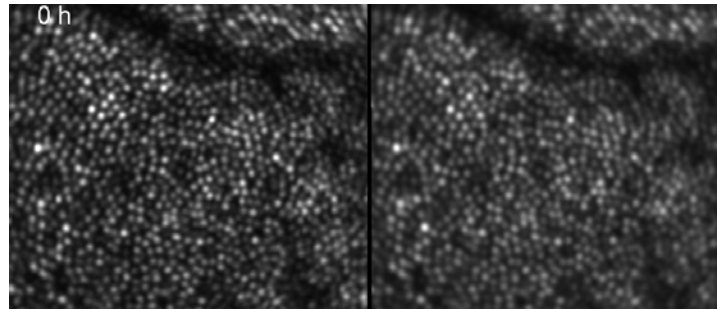


Fig. 10. First frame of a movie (Media 5) showing intensity fluctuations in depth integrated OCT (left) and SLO (right) images of cone photoreceptors within 96 hours (image extension: $\sim 0.88^\circ \times 0.75^\circ$, retinal eccentricity: $\sim 4^\circ$ nasal from the fovea)

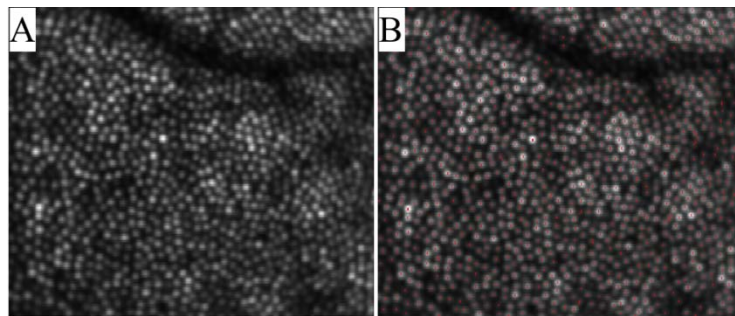


Fig. 11. Over an extended measurement period (96 hours) averaged depth integrated OCT images of cone photoreceptors (A) and corresponding cone locations (B) (Image extension: $\sim 0.88^\circ \times 0.75^\circ$, retinal eccentricity: $\sim 4^\circ$ nasal from the fovea)

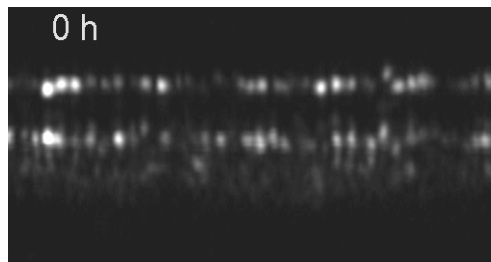


Fig. 12. Frame 1 of a movie (Media 6) showing a representative B-scan over the entire measurement period (96 hours). Image extension: $\sim 0.88^\circ \times 120\mu\text{m}$, retinal eccentricity: $\sim 4^\circ$ nasal from the fovea)

Figure 12 shows a representative B-scan of this measurement series. At the IS/OS junction large intensity variations can be observed (in comparison to Fig. 4), however, the position of the cones at this layer stays constant over time. On the other hand, beside the large intensity fluctuations small changes in the depth position of the cone reflections at the ETPR layer can be observed. Since the registration between the individual data sets is better than the extension

of a cone (transverse) and better than the coherence length of the light source (in depth, as can be observed at the IS/OS junction and in Fig. 10) we believe that this change in position corresponds to different phases within the renewal process of each individual cone that is captured at different measurement times. At the IS/OS junction new OS disks are generated and from time to time the RPE sheds disks at the distal end of the cones (the position of the ETPR). The shed disks are then disintegrated by phagocytosis within the RPE. Both processes differ considerably in their dynamics because the generation of new disks is a continuous process while the phagocytosis is not. According to animal studies that counted the number of phagosomes at different day times the incidence of phagocytosis can be significantly different throughout the day [14]. Therefore, depending on the time delay between the last event of disk shedding and the measurement of each individual cone, different OS lengths can be observed because the number of newly generated disks since this event is different. It should be noted here, that different OS lengths could be observed in the 7 hour experiment as well, however during the 7 hours the lengths remained constant.

Recently we reported on BRS that appeared within the OS of cone photoreceptors, however, at that time the origin of these BRS remained somehow unclear. The time series will shed some light on this issue. Figure 13 shows a representative B-scan containing BRS. As can be observed in the movie one BRS appears at the measurement time of 48 hours shortly beneath the IS/OS junction and moves in the last two frames towards the ETPR layer. Several of these BRS showing this time evolution can be found in this data set as well as in the data sets of other volunteers. We hypothesize that this BRS originates from a crack or defect within the OS segments that gives rise to a refractive index mismatch and therefore to a signal in the OCT image. Because of the cone OS renewal this crack or defect moves towards the ETPR layer (new discs are generated at the IS/OS layer and “old” discs are removed by the RPE at the ETPR layer). Interestingly one BRS can be seen in the movie that appears in the first frame, disappears in the second and reappears in the last frames. However, in contrast to the moving BRS no distinct signal from the ETPR layer can be observed at the position of this cone. Therefore it is more likely that this BRS does not correspond to a crack or defect in the OS but to the end tip of a shorter cone.

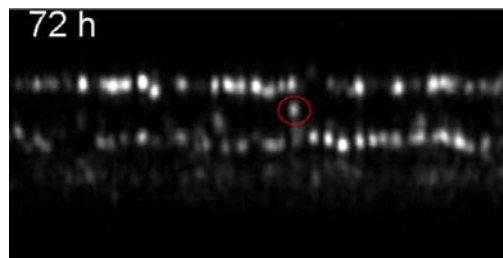


Fig. 13. Frame 4 of a movie (Media 7) showing a representative B-scan over the entire measurement period (96 hours) containing a BRS that appears at 48 hours. The BRS is marked with a circle. Image extension: $\sim 0.88^\circ \times 120 \mu\text{m}^2$, retinal eccentricity: $\sim 4^\circ$ nasal from the fovea)

Similar to the first short term experiment we measured the OS length of each detected cone. As can be seen in Fig. 14 the thickness distribution is the same for all days and is similar to the one presented in Fig. 8 (7 hours measurement). However, the standard deviation (SD) of the length measurements differs from the one in Fig. 8. First of all the peak of the SD distribution is at a larger SD than in the previous experiment. This can be explained by the small length changes (differing ETPR positions) observed in Figs. 12 and 13. On the other hand a second, smaller peak of the distribution is visible at around $16 \mu\text{m}$ which we attribute to the moving BRS within the data set. We manually counted all BRS that showed motion in at least 3 of the 5 frames and measured the position of each BRS. Out of the 961 cones detected (c.f. Figure 11), 51 BRS showed motion in at least 3 frames. Figure 15 shows the change in the distance between the IS/OS junction and the position of BRS measured in volunteer 1. For

each of these the change in position was fitted with a straight line and the slopes of all fits were averaged to obtain a mean OS growth rate. With this procedure we measured a mean OS growth rate of (110 ± 40) nm per hour for volunteer 1 and (110 ± 50) nm/h for volunteer 2, respectively. These growth rates are in excellent agreement with animal studies [23,24] and the AO-ophthalmoscope method [15]. Finally, we evaluated the intensity fluctuations for the long term measurement. Although the intensity distribution within the images is similar to the previous experiment (c.f. Figure 16A), the increased relative changes indicated by the much broader distributions and the shift of the peak of the distribution to the right in Fig. 16 B is evident.

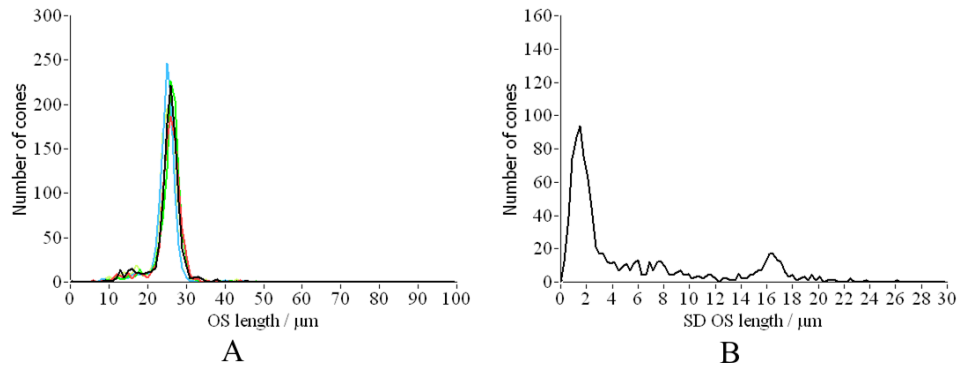


Fig. 14. A) Distribution of cone outer segment lengths for each day (corresponding to different colors). B) Distribution of standard deviations calculated over the whole measurement period.

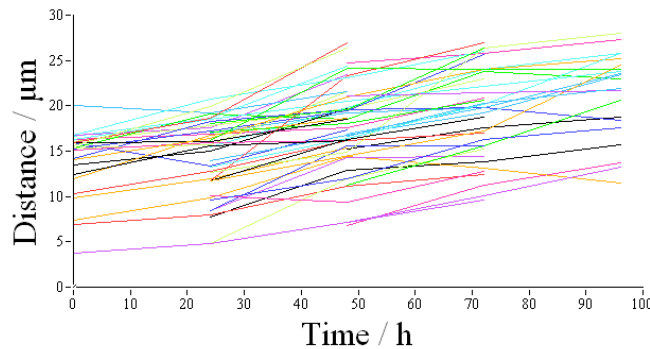


Fig. 15. Change in depth position (distance IS/OS to BRS) of all BRS that showed motion in at least 3 frames of the 96 hours measurement series of volunteer 1. The different colors correspond to different BRS.

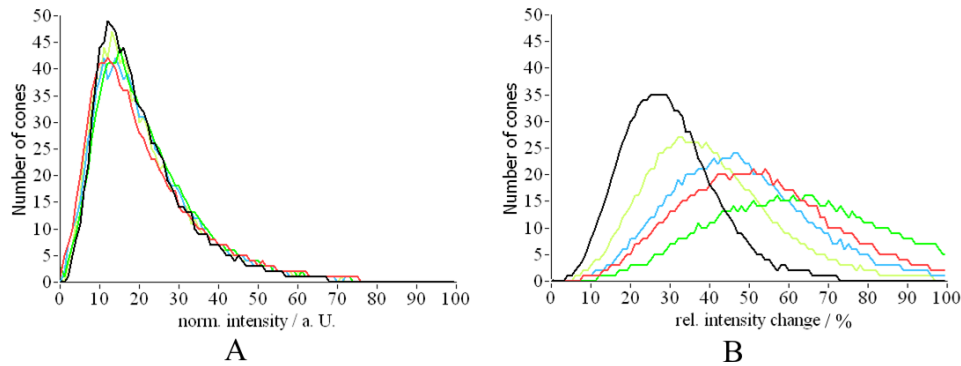


Fig. 16. A) Distribution of backscattered intensity of individual cones (colors correspond to different measurement times). B) Relative intensity variation (normalized by the average intensity retrieved from each layer) over time of cones for individual retinal layers (black depth integrated intensity, red IS/OS junction, green OS, blue ETPR, yellow RPE).

4. Discussion and conclusion

We demonstrated the performance of our SLO/OCT instrument to image and observe *in vivo* the three dimensional structure of human cone photoreceptors over extended periods of time. This observation is only possible because the registration between the recorded 3D data sets is better than the extension of a cone (transverse) and better than the coherence length of the light source (in depth). We investigated changes in the backscattered intensity of individual cones and at different retinal layers for two different time periods: 7 hours and 96 hours, respectively. Previous studies investigated intensity fluctuations using AO-FC [19] which showed similar results as our SLO and depth integrated OCT images. However, our study showed that intensity fluctuations within individual retinal layers (IS/OS, OS, ETPR, RPE) are much more pronounced than in the depth integrated image (that was investigated using AO-FC). Interestingly, we found that the intensity fluctuations within a cone at the IS/OS and the ETPR are rather independent from each other (c.f. Figure 3). Therefore we can now directly confirm the suggestion made in Ref [19] that a change in the pointing direction of a cone cannot be the origin of these intensity fluctuations because in that case the intensity at both layers would be affected similarly. In Ref [19] it is speculated that the intensity changes mainly origin from the reflection at the ETPR. However, our results show that in both layers intensity fluctuations can be observed. The origin of these intensity fluctuations remains therefore unclear. Nevertheless we think that the intensity fluctuations at the IS/OS could be caused by the permanent generation of new discs at the IS/OS layer which may result in a change of the refractive index difference at this interface. Depending on the phase within the disc generation process high or low backscattering signal is observed. Noticeable is that the BRS (located within the OS) do not change their intensity within the 7 hours period. This strengthens the above mentioned hypothesis that the intensity fluctuations are caused only by changes that affect the interface between inner and outer segments of cone photoreceptors. Similar, the intensity fluctuations observed at the ETPR could be explained by different status of the disc shedding process. However, within the 7 hours period no change in the OS length is observed (in contrast to the 96 hours measurement) therefore it is most likely that during this period discs from the majority of the cones were not shed. Although there is no data on human cone disc shedding, results from animal studies show that in some species the shedding process is determined by a circadian rhythm [25–28] with a peak of disc shedding shortly after light onset [14], a period that has not been investigated in our study. Note that the OS length changes observed in the 96 hour experiment are very small (up to a few μm) which is in agreement with the observed size of phagosomes (that would correspond to the expected length changes) in animal studies [13].

Still unclear is the origin of bright reflections at the transverse location of individual cones within the RPE (c.f. movie in Fig. 3) that are changing with time. Although we can, at the current state of investigation, only speculate on the origin, it might be plausible that light is backscattered at migrating macrophages (probably containing phagosomes) or pigments. Depending on the position of these particles in respect to the overlying cone, light can be back-coupled into the photoreceptor which finally leads to our observation. Interestingly, the cones under which these reflections can be observed are randomly changing. Although at the depth location of the RPE (depth integrated over $12\mu\text{m}$ around the peak of the RPE) each en-face image shows a random pattern (c.f. Figure 4) the full cone mosaic can be observed when all images recorded over the measurement period of 7 hours are averaged (c.f. Figure 17). This strengthens the assumption that light originating from this layer is back-coupled through the photoreceptors (at least at some points in time).

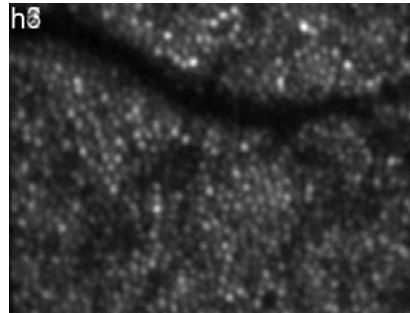


Fig. 17. En-face image of the RPE, averaged over the measurement period of 7 hours (depth integrated $12\mu\text{m}$ around the peak of the RPE position) OCT images. (Image extension: $\sim 0.94^\circ \times 0.7^\circ$, retinal eccentricity: $\sim 4^\circ$ nasal from the fovea)

As shown in Fig. 13 the previously reported BRS [16] are changing their position within the OS when imaged over an extended period of time (96h). Although we hypothesize that the BRS originate from defects or cracks within the packing of the OS discs, a proof of this hypothesis is very challenging. Animal studies including histology or in vitro multi-photon imaging could probably be of help here, although a perfect registration between the different methods might be very difficult.

The measured motion speed of the BRS corresponds well with the cone renewal speed known from animal studies [23,24] and from AO-FC measurements [15]. Note that both in vivo methods do require measurement series over several time points. While our method measures the renewal speed over an extended time (5 measurements in 96h), the AO-FC method requires several measurements with shorter time intervals (every 15 minutes up to a total time of 5 hours). Therefore two (probably?) different renewal speeds are measured. With our method a mean renewal speed (averaged over 4-5days) is measured while with the AO-FC method a renewal speed within 5 hours is measured.

Finally we want to point out that the results presented in this paper are based on 2 volunteers. Certainly more subjects have to be imaged in order to strengthen the presented hypotheses.

Acknowledgments

Financial support from the Austrian Science Fund (FWF grants P19624-B02 and P22329-N20) is acknowledged. The authors acknowledge discussions with P. K. Ahnelt from the Medical University of Vienna and D. R. Williams from the University of Rochester.